

ATOMIUM: ALMA Tracing the Origins of Molecules In dUst-forming oxygen rich M type stars

1

Leen Decin (KU Leuven), Carl Gottlieb (CfA)¹, Anita Richards (Manchester UK), and the ATOMIUM team²

ATOMIUM web page:

<https://fys.kuleuven.be/ster/research-projects/aerosol/atomium/atomium>

The official *Landing Page* can be accessed via the ‘almascience pages: Large Programs’ under the Data tab.³

A. Goals:

- (i) Morpho-Kinematical and Chemical properties of the winds
- (ii) Density Structures / Wind Structures
- (iii) Reciprocal Dynamical and Chemical Properties of the Winds
- (iv) Gas — Dust phase change
- (v) Chemical Pathways

B. Specifications:

14 AGBs and 3 RSGs → 12 oxygen rich AGBs, 3 oxygen rich RSG, and 2 S-type AGBs

6 Pulsation types

- 27 GHz wide homogeneous spectral line surveys
- ~50 antennas
- 3 configurations of the ALMA array: Compact (~1"), Mid (0.20"), and Extended (25 - 50 mas)
- MAS: ~25 mas — 8"

Cycle 6

Alotted time: 113 hours

Band 6 (214 – 270 GHz)

Spectral resolution 1.3 km/s

Sensitivity 1.5 – 5 mJy/beam

Angular resolution 50 mas—10"

Carl Gottlieb

17 April 2024

¹ CGOTTLIEB@CFA.HARVARD.EDU

² The ATOMIUM team consists of about 45 scientists: most are in Europe except 4 in the US.

³ The exact link depends on which region you are in as it points to the local archive mirror.

C. Background:

C.1: The example of the Mira variable IK Tau Abridged Reference list

Reference	Angular Resolution	Frequency Band
SINGLE ANTENNA:		
Kim et al. (2010)	18'' – 20''	7
Decin et al. (2010)	10'' – 25''	6 & 7
De Beck et al. (2013)	16'' – 26''	6 & 7
SMA:		
De Beck et al. (2013)	0.9''	7
ALMA:		
Decin et al. (2017)	150 mas	7
Decin et al. (2018)	150 mas	7
VLT/SPHERE-ZIMBOL:		
Adam & Ohnaka (2019)	20 - 30 mas	\gtrsim 646 nm

References:

[Kim et al. \(2010\)](#)
[Decin et al. \(2010\)](#)
[De Beck et al. \(2013\)](#)
[Decin et al. \(2017, 2018\)](#)
[Adam & Ohnaka \(2019\)](#)

Foundational:

R Dor and IK Tau in Band 7 (335 – 360 GHz) [Decin et al. \(2017, 2018\)](#)

ATOMIUM:

Overview: [Gottlieb et al. \(2022\)](#)
General summary: [Decin et al. \(2022\)](#)
VLT/SPHERE: [Montargès et al. \(2023\)](#)

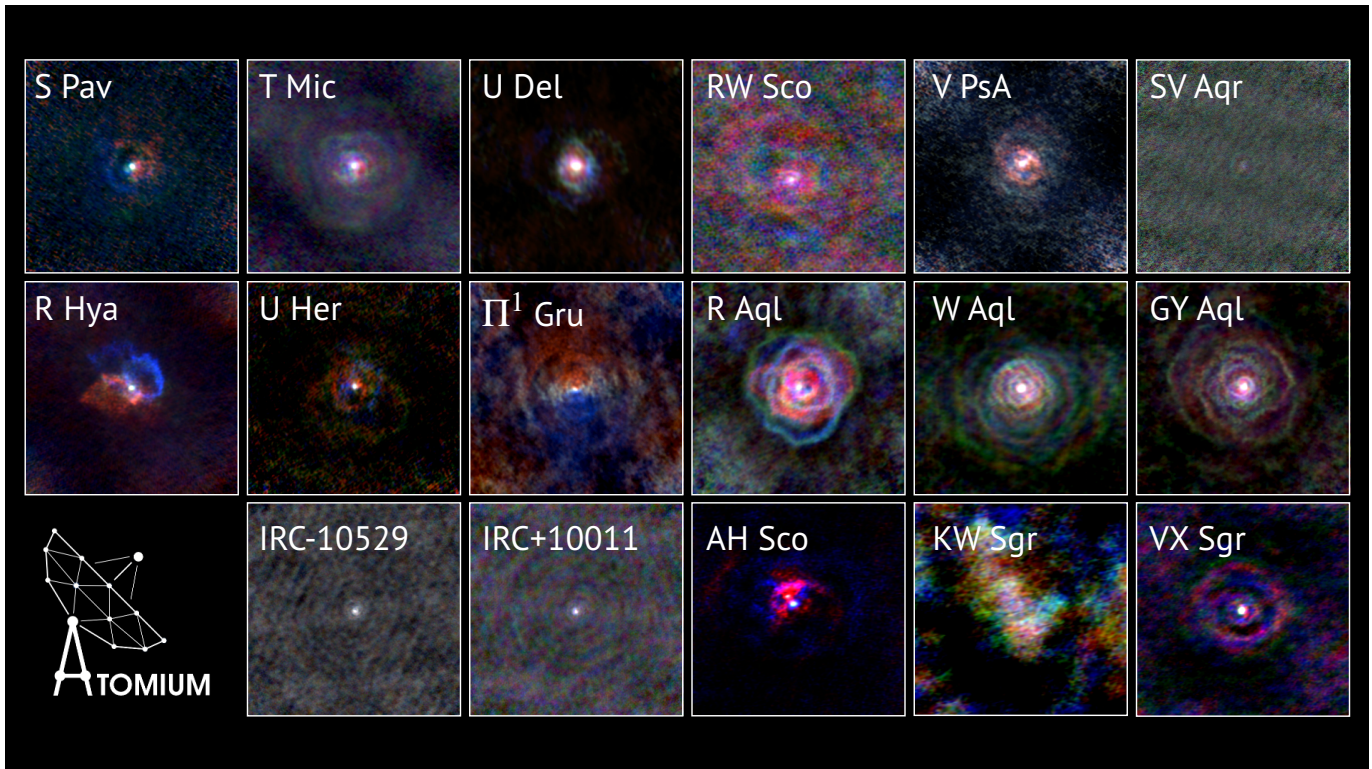


Figure 1. Gallery of AGB winds derived from the channel maps of the $^{12}\text{CO } J = 2 \rightarrow 1$ emission in the 14 AGB stars and 3 RSG stars observed in ATOMIUM which is separated into three velocity intervals. Emission that is redshifted with respect to the LSR is in **red**, blueshifted emission is in **blue**, and emission centered on the systemic velocity is in **white**. The scale bars denote an angular extent of $1''$.

A. Method:

The prevailing wind morphology of each star was classified in a stepwise approach described in the *Supplementary Materials* in [Decin et al. \(2020\)](#)

B. Observation: ([Decin et al. 2020](#))

- Observed morphologies are best described as: Spiral-like, Bipolar, or an EDE/Disk
- Morphologies of the AGB stars mirror the shape(s) of the PNe

C. Hypothesis: (Sub)stellar companions shape the winds of evolved stars

C.1 Hydrodynamical simulations:

([El Mellah et al. 2020](#); [Maes et al. 2021](#); [Malfait et al. 2021](#); [Esseldeurs et al. 2023](#))
Binary separation, wind velocity, companion mass

C.2 In-depth studies of the morphology:

- (i) S-type star π^1 Gru ([Homan et al. 2020](#))
- (ii) Semiregular variable R Hya ([Homan et al. 2021](#))

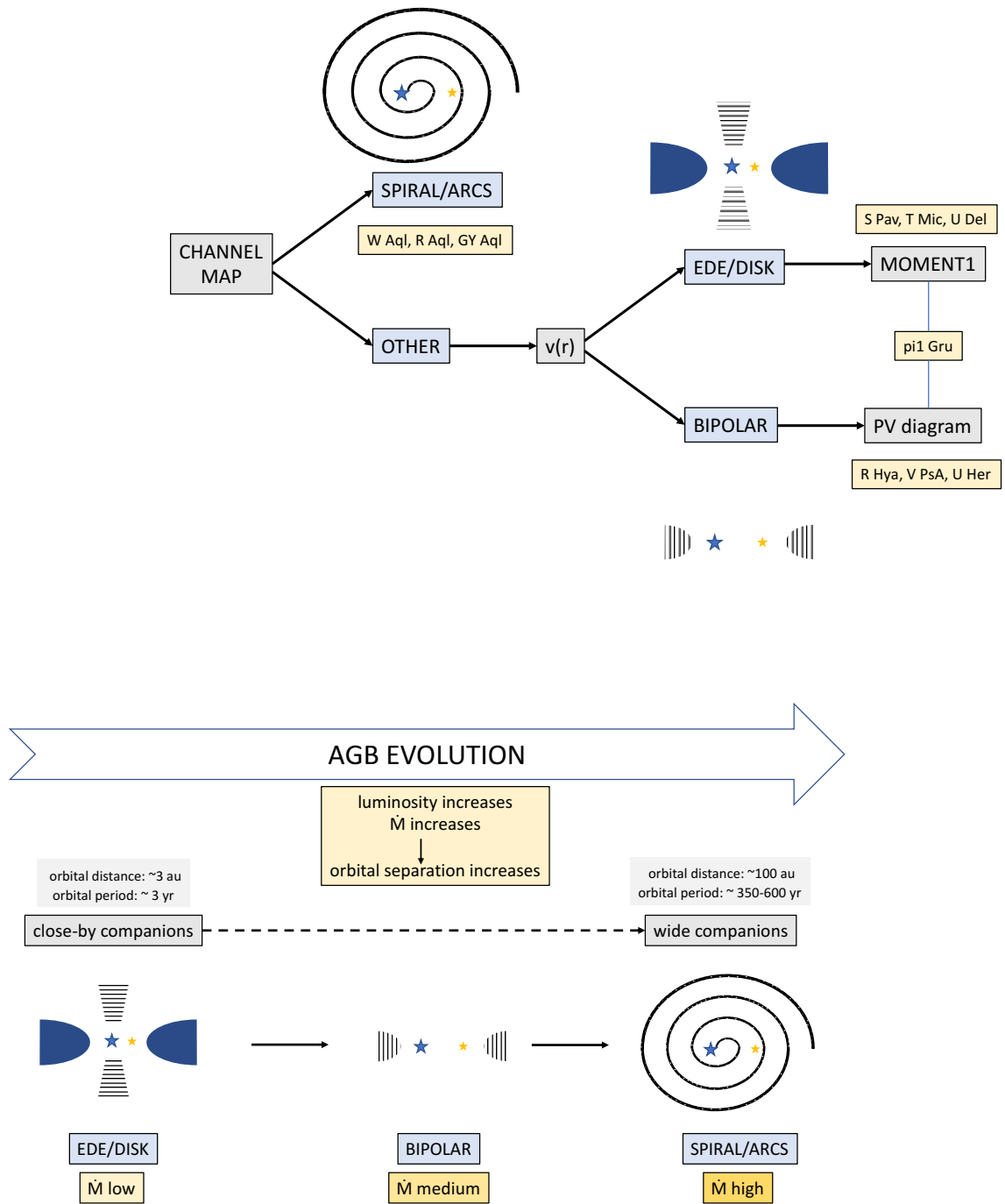


Figure 2. *Upper:* Schematic diagram illustrating the steps entailed in classifying the morphologies of the ATOMIUM sources by Decin et al. (2020). *Lower:* Diagram illustrates the evolution of the wind morphology during the AGB phase.

A. General

Wallström et al. (2024) : 24 molecules, ~300 rotational lines, ~30 lines unassigned

Source	Ubiquitous	SO, SO ₂	S bearing	H ₂ O, OH	Dust precursors	Halides
Semiregular variable stars:						
R Dor	CO, HCN, SiO	SO, SO ₂	SiS, CS	H ₂ O, OH	..., TiO, AlO, AlOH, TiO ₂	AlCl
U Del	CO, HCN, SiO			H ₂ O		
V PsA	CO, HCN, SiO	SO, SO ₂		H ₂ O		
T Mic	CO, HCN, SiO	SO, SO ₂	CS	H ₂ O, OH	PO, TiO, AlO	
S Pav	CO, HCN, SiO	SO, SO ₂		H ₂ O, OH	PO, TiO, AlO	
Mira variable stars:						
R Hya	CO, HCN, SiO	SO, SO ₂	CS	H ₂ O, OH	PO, TiO, AlO	
U Her	CO, HCN, SiO	SO, SO ₂	SiS, CS	H ₂ O, OH	PO, TiO, AlO, AlOH	AlF
R Aql	CO, HCN, SiO	SO, SO ₂		H ₂ O, OH	PO, TiO, AlO	
GY Aql	CO, HCN, SiO	SO, SO ₂	SiS, CS, H ₂ S	H ₂ O	PO, TiO, AlO, AlOH	AlCl
IK Tau	CO, HCN, SiO	SO, SO ₂	SiS, CS	H ₂ O, OH	..., TiO, AlO, AlOH, TiO ₂	NaCl
OH/IR stars:^(b)						
RW Sco	CO, HCN, SiO	SO, SO ₂	SiS, CS	H ₂ O	PO	
IRC-10529	CO, HCN, SiO	SO	SiS	H ₂ O	PO, TiO, AlO, AlOH	KCl, NaCl, AlF
IRC+10011	CO, HCN, SiO	SO, SO ₂	SiS	H ₂ O	PO, TiO, AlO, AlOH	KCl, NaCl, AlF
Long period variable LPV:						
SV Aqr	CO, HCN, SiO	SO, SO ₂		H ₂ O		
S-Type stars:						
π^1 Gru	CO, HCN, SiO		SiS			
W Aql	CO, HCN, SiO		SiS, CS		[CN, HCCCN, SiN, SiC, SiCC] ^(a)	AlCl, AlF
Red supergiants RSG:						
AH Sco	CO, HCN, SiO	SO, SO ₂	SiS, CS, H ₂ S	H ₂ O, OH	PO, TiO, AlO, AlOH	AlF
KW Sgr	CO, HCN, SiO	SO		H ₂ O		
VX Sgr	CO, HCN, SiO	SO, SO ₂	SiS, CS, H ₂ S	H ₂ O, OH	PO, TiO, AlO, AlOH, TiO ₂	AlF, NaCl?

	\dot{M}	CO	HCN	SiS	CS	AlF	KCl	NaCl	H ₂ S	AlOH	AlO	SO	SO ₂	H ₂ O	PO	TiO	OH	SiO
S Pav	1.3e-07	3	2	0	0	0	0	0	0	0	0	4	35	8	4	3	4	14
RW Sco	1.3e-07	2	2	3	1	0	0	0	0	0	0	4	18	2	2	0	0	10
T Mic	1.4e-07	2	2	0	1	0	0	0	0	0	1	7	21	6	2	0	4	11
R Hya	1.8e-07	3	6	0	1	0	0	0	0	0	1	8	36	10	4	9	4	14
SV Aqr	2.7e-07	1	1	0	0	0	0	0	0	0	0	3	7	1	0	0	0	6
U Her	3.2e-07	3	4	5	1	1	0	0	0	1	2	8	39	6	2	0	0	11
U Del	3.7e-07	2	1	0	0	0	0	0	0	0	0	0	0	1	0	0	0	6
V PsA	4.8e-07	2	1	0	0	0	0	0	0	0	0	2	2	2	0	0	0	11
pi1 Gru	9.2e-07	3	6	25	0	0	0	0	0	0	0	0	0	0	0	0	0	11
R Aql	1.6e-06	3	2	0	0	0	0	0	0	0	2	2	26	7	2	3	4	14
GY Aql	2.3e-06	3	2	11	2	1	0	2	1	2	2	7	16	3	2	3	0	10
W Aql	2.7e-06	4	10	45	2	2	0	0	0	0	0	0	0	0	0	0	0	12
KW Sgr	3.6e-06	2	2	0	0	0	0	0	0	0	0	2	0	1	0	0	0	9
AH Sco	1.0e-05	3	6	5	1	1	0	0	1	1	3	11	63	6	4	6	2	12
IRC-10529	1.0e-05	4	2	21	2	1	5	7	1	0	2	5	11	6	4	0	0	12
IRC+10011	1.9e-05	3	4	22	2	1	5	8	1	2	1	6	12	8	4	2	0	13
VX Sgr	6.0e-05	3	6	9	2	1	0	0	1	2	4	12	66	7	2	7	4	11

Figure 3. The Table lists the number of rotational lines that were detected in each molecule in the 17 ATOMIUM sources. The sources are listed in order of increasing mass loss rate (\dot{M}). The Table does not include molecules which were identified in only a single source (Wallström et al. 2024).

B. Outflowing Wind:

Tom Millar (Queens Univ. Belfast UK), Marie Van de Sande (Leiden NL)

References:

Van de Sande & Millar (2022) Affect of UV radiation from a stellar companion on the abundances of carbon bearing and oxygen bearing species in outflowing winds

Maes et al. (2023) Abundances of 12 parent species in oxygen rich sources, and 13 species in carbon rich sources as a function of temperature & density in the outflowing winds

C.1 Observations:

TiO and OH maps (see Fig. 6)
 TiO + OH \rightarrow TiO₂ Plane (2013)

Abundance ratios:

OH/H₂O $\sim (0.7 - 2.8 \times 10^{-2})$ Baudry et al. (2023)
 OH/TiO $\sim (1 \times 10^3 - 1 \times 10^4)$ Baudry et al. (2023); (This work)
 TiO \sim photospheric abundance at $r \lesssim (2 - 3) R_\star$ in R Dor (Danilovich et al. 2020)

Column densities general:

TiO/OH ratio: Comparable in 2 SRs (R Dor & SPav) & 2 Miras (R Hya & R Aql)
 TiO and AlO: Comparable in R Dor, R Hya, and R Aql
 AlO/TiO $\lesssim 3$ This work
 AlOH/AlO ~ 3 in R Dor This work (sensitive to H/H₂ ratio, Gobrecht et al. 2022)

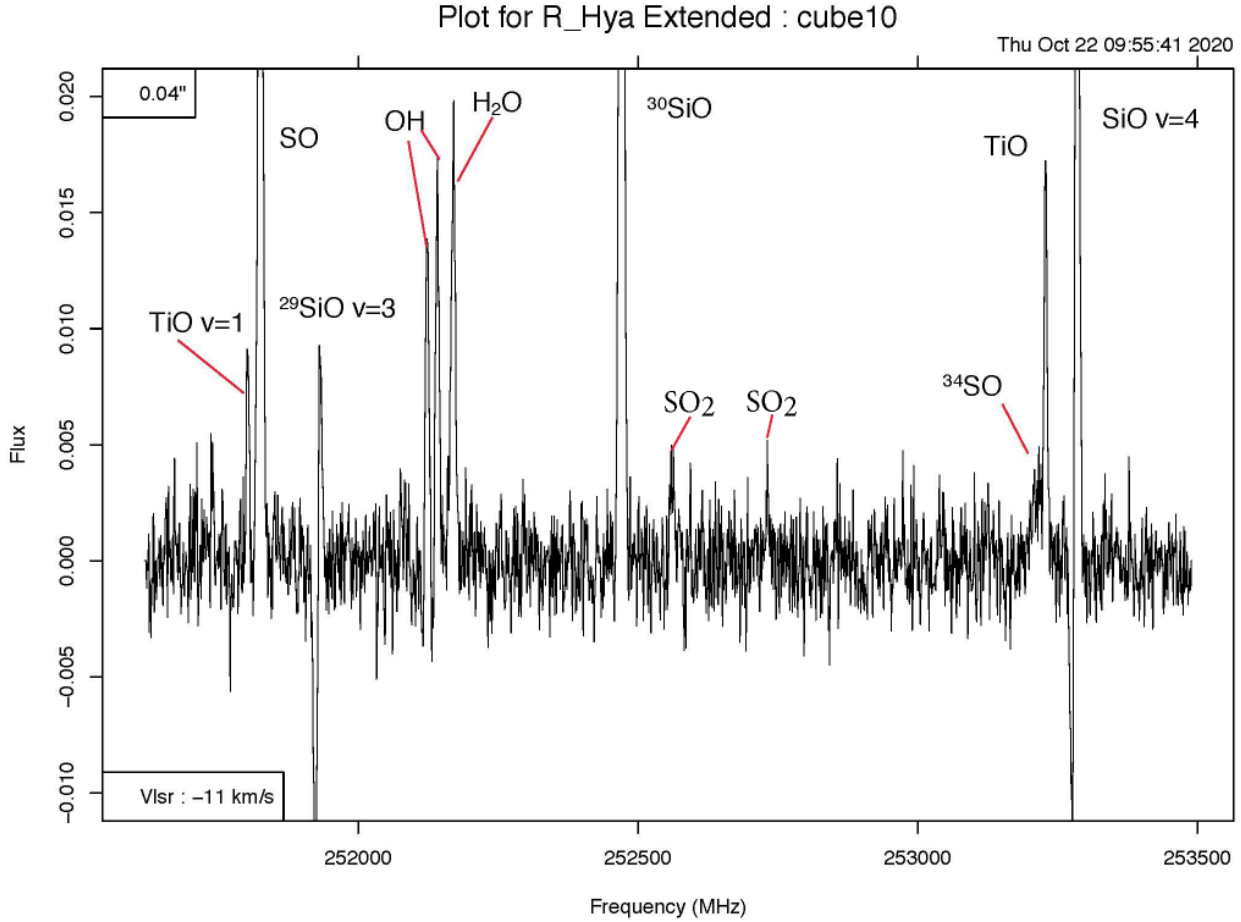


Figure 4. Spectrum of R Hya in Cube 10 observed in the Extended configuration. Present in the spectrum are lines of: **AlOH $J = 8 - 7$ + TiO $v = 1$ $^3\Delta_1$ $J = 8 - 7$** ; SO ($v = 0$) $N, J = 6, 5 - 5, 4$; ²⁹SiO ($v = 3$) $J = 6 - 5$; OH ($v = 0$) $^2\Pi_{3/2}$ $J, F = 29/2, 14 - 29/2, 14$; OH ($v = 0$) $^2\Pi_{3/2}$ $J, F = 29/2, 15 - 29/2, 15$; H₂O (100-020) $7_{4,3} - 8_{5,4}$; ³⁰SiO ($v = 1$) $J = 6 - 5$; SO₂($v = 0$) $J_{K_a, K_c} = 32_{4,28} - 31_{5,27}$; SO₂($\nu_2 = 1$) $J_{K_a, K_c} = 15_{2,14} - 15_{1,15}$; ³⁴SO ($v = 0$) $N, J = 6, 6 - 5, 5$; TiO ($v = 2$) $^3\Delta_2$ $J = 8 - 7$; TiO ($v = 0$) $^3\Delta_1$ $J = 8 - 7$; and SiO ($v = 4$) $J = 6 - 5$.

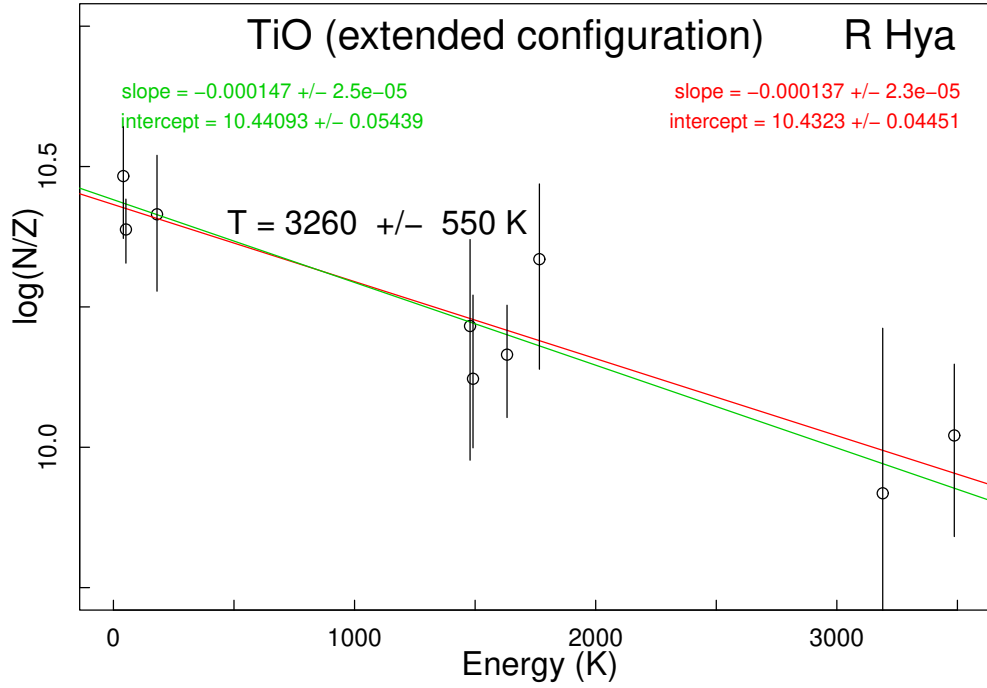


Figure 5. Vibrational temperature (VT) diagram of TiO derived from observations of R Hya in the Extended configuration extracted with an aperture of 80 mas diameter. The VT diagram was constructed with lines of TiO in the $N = 7 - 6$ and $8 - 7$ transitions observed in spw 02, 03, 10, and 11. The rotation-vibration partition function (Z) of TiO at T_{vib} is from McKemmish et al. (2019, and references therein).

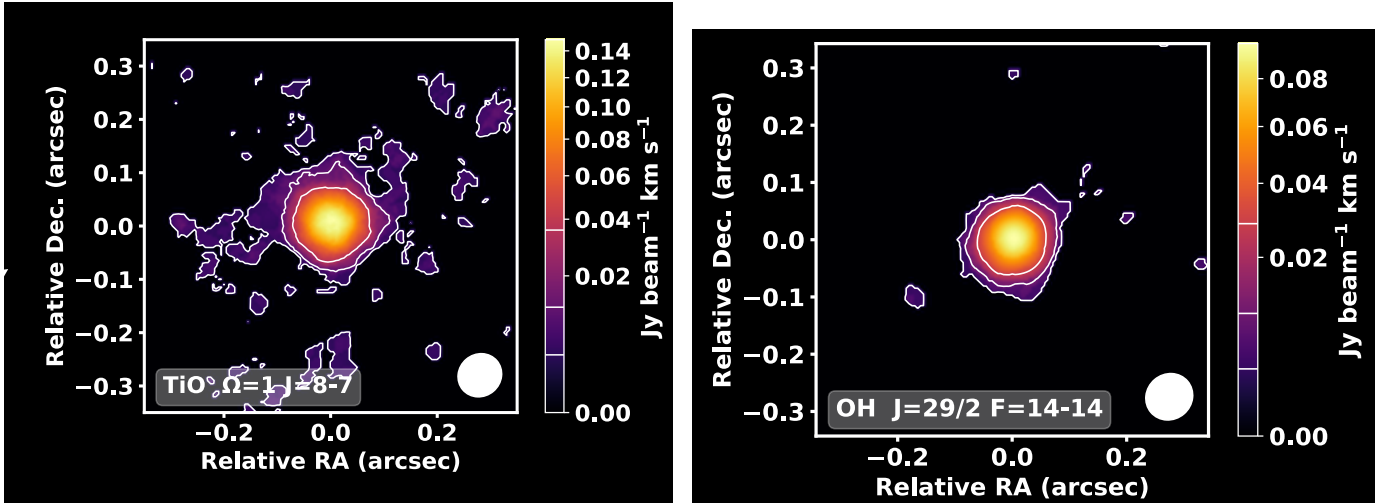


Figure 6. Moment 0 maps of TiO (*left*) and OH (*right*) observed in R Hya ($R_{\star} = 23$ mas) in the extended configuration and extracted with an aperture of 20 mas. The maps were computed from the combined dataset (Decin et al. 2022). The white contours are 3, 10, and 30 times the noise in the integrated intensity maps. The $J = 8 - 7$ transition in the ${}^3\Delta_1$ state of TiO at 253,229.033 MHz is 22 MHz higher in frequency than the much weaker $N_J = 6_6 - 5_5$ transition of ${}^{34}\text{SO}$ at 253,207.017 MHz (see Fig. 4).

C2. Chemistry

John Plane (Leeds UK)

Plane (2013)

Plane & Robertson (2022)

David Gobrecht (Gothenburg Sweden)

Gobrecht et al. (2022) Al_2O_3 clusters in R Dor: $\text{AlO} + \text{H}_2 \longleftrightarrow \text{AlOH} + \text{H}$; H/H_2 ratio

Gobrecht et al. (2023) Mg and Ca aluminate clusters: MgAl_2O_4 and CaAl_2O_4

AlOH/AlO ratio predicted by Gobrecht et al. (2022) is comparable to the (revised) measured ratio (This work).

C3. Gas-Dust interaction

Shown here are the images of the dust observed with VLT/SPHERE by Montargès et al. (2023) in SPav and RAql on this page, and RHya in Fig. 8. A detailed comparison of the TiO emission observed in ATOMIUM with these images of the dust is in progress (This work).

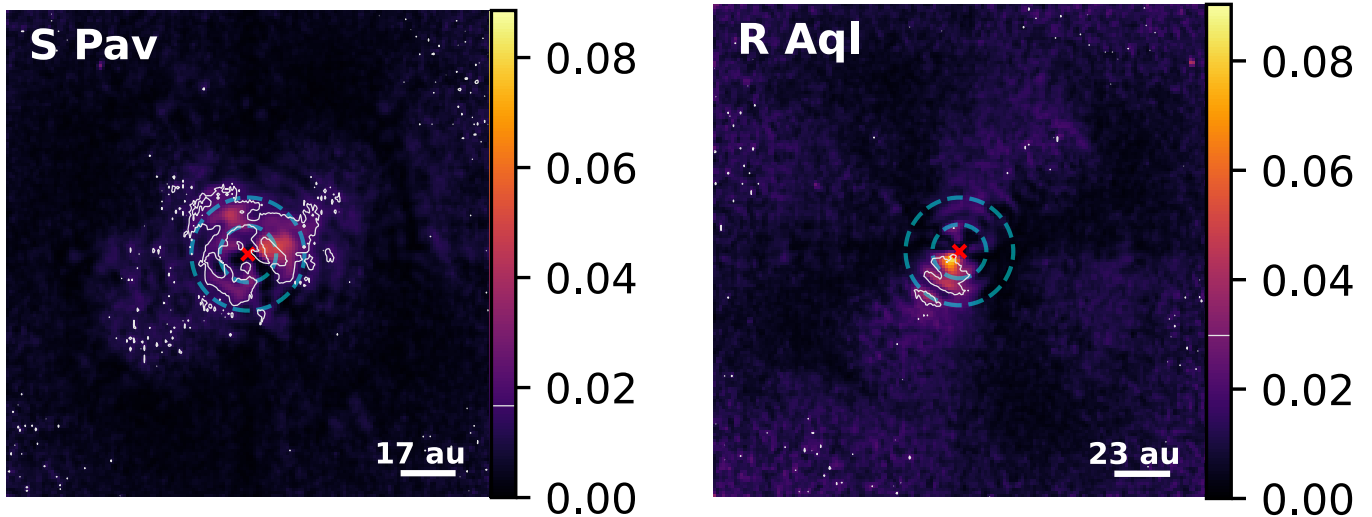


Figure 7. DoLP (degree of linear polarization) of the dust in SPav ($R_\star = 6$ mas) and RAql ($R_\star = 6$ mas) observed at an angular resolution of 25 – 30 mas with VLT/SPHERE-ZIMBOL by Montargès et al. (2023). The observations of the dust here, the one in RHya in Fig. 8 also by Montargès et al., and prior observations by others establish that dust formation occurs at very specific sites in the inner wind. The dashed circles refer to the distances of $20 R_\star$ and $10 R_\star$ from the star. The white contours correspond to the 5σ level of the DoLP.

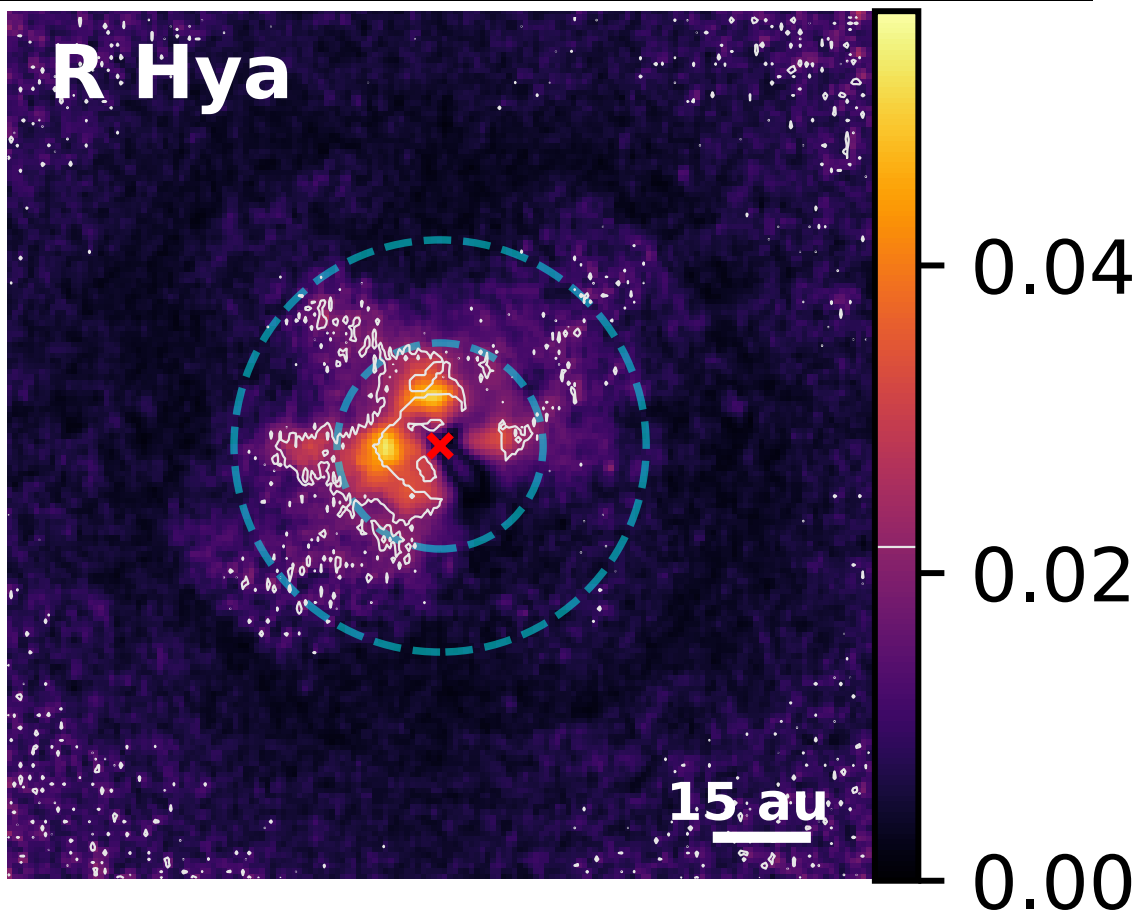
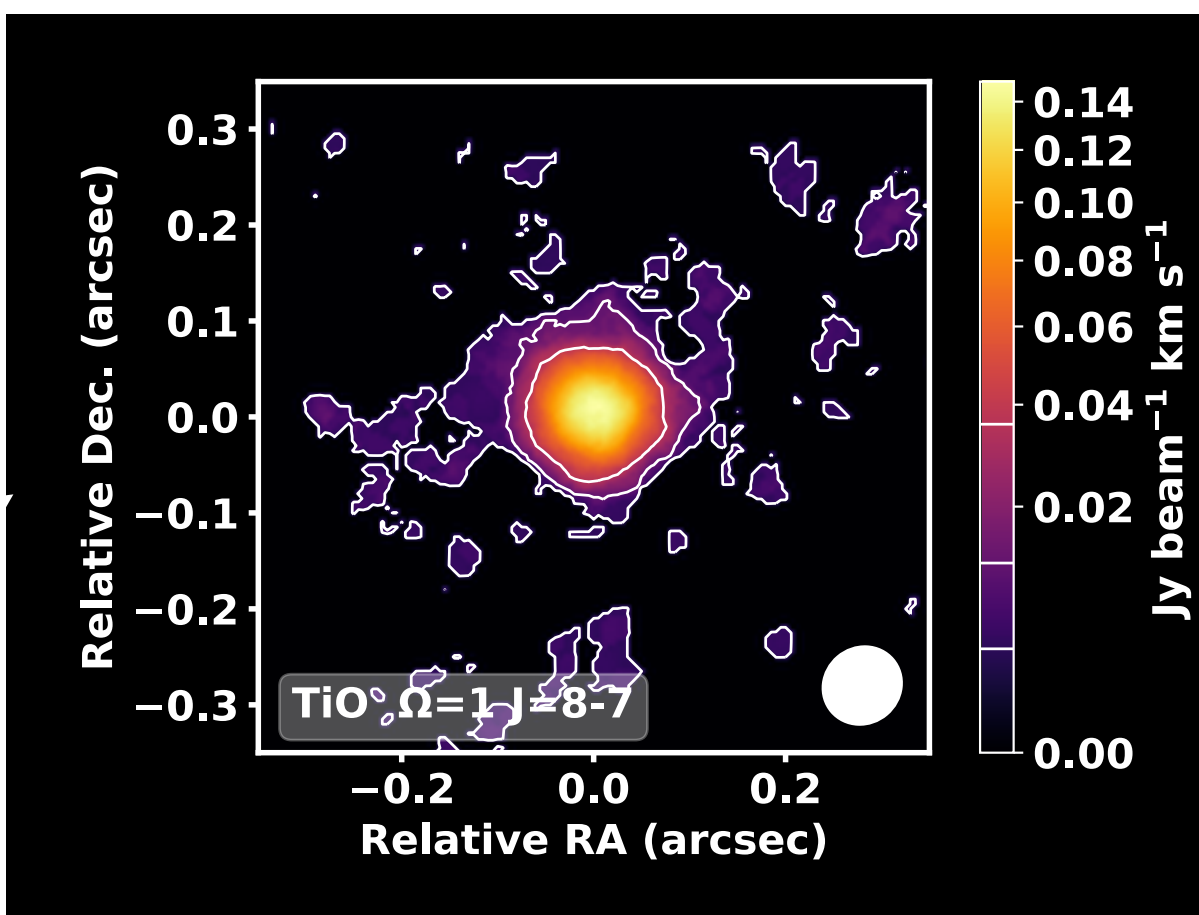


Figure 8. See the Fig. 7 caption. The scales in the two plots are similar, but they are not identical: $20 R_{\star}$ in the *Lower* plot is ≈ 230 mas in the *Upper* plot.

The parameter β in the velocity law (Lamers & Cassinelli 1999)

$$v(r) = v_0 + (v_\infty - v_0) \left(1 - \frac{r_{\text{dust}}}{r}\right)^\beta \quad (1)$$

is empirically constrained, although β has some theoretical support (see Sect. 5.1 in Gottlieb et al. 2022, and references therein). The dust condensation radius (r_{dust}) is $2 - 3 R_\star$ in most of the stars in the ATOMIUM survey. The only exceptions are U Del ($r_{\text{dust}} = 5.1 R_\star$); and IK Tau with either $r_{\text{dust}} = 6.3 R_\star$ in Decin et al. (2018), or $r_{\text{dust}} = 8.6 R_\star$ in Gottlieb et al. (2022). The possible connection between the velocity parameter β and the composition of the dust in the inner wind (via the SE index) had been considered previously (see Höfner & Olofsson 2018; Decin 2021, and references therein), and is discussed in some detail.

This work: $\text{SE} \leq 2$ and $\beta \leq 1$ in R Dor, T Mic, S Pav, and R Hya.

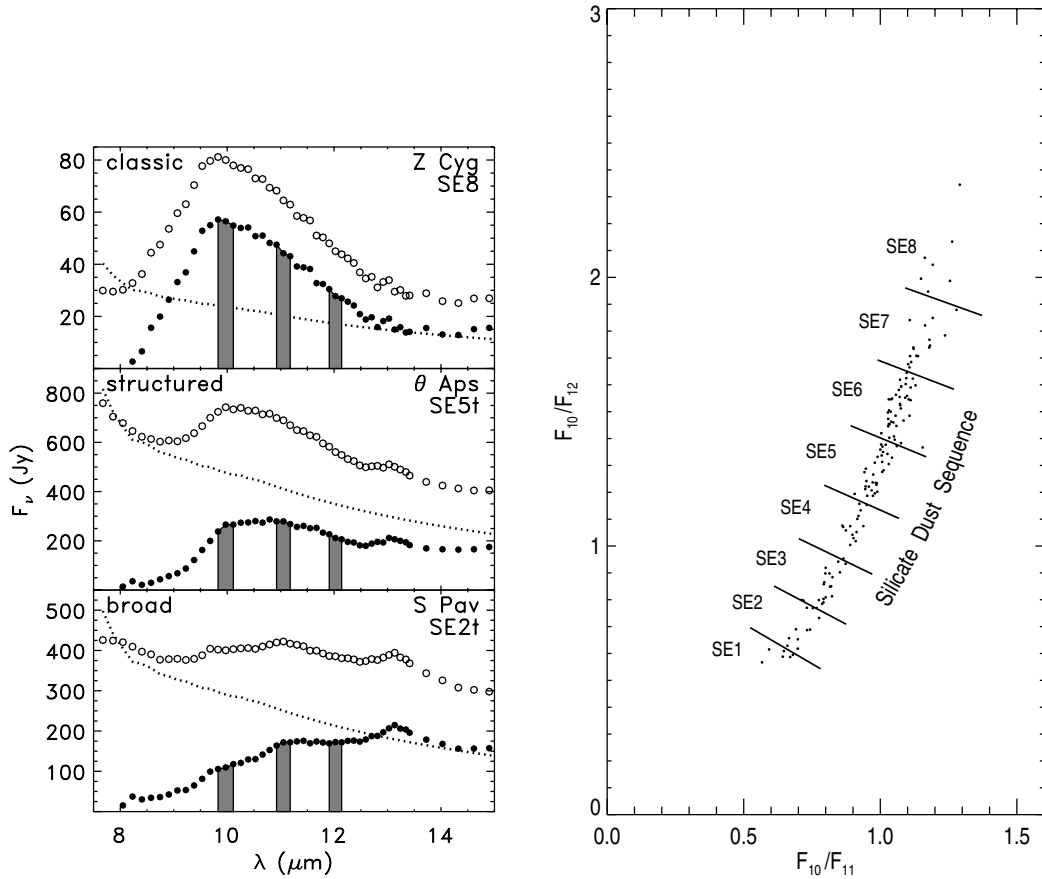


Figure 9. The Plots and the Figure captions are from Egan & Sloan (2001).

Left: Sample spectra for **classic silicate** emission (top), **structured silicate** emission (middle), and **broad oxygen-rich** dust emission (bottom). In each panel, the *open circles* refer to the total spectrum (star + dust), the *dashed line* is the fitted stellar continuum, and the *filled circles* refer to the dust emission after subtracting the stellar continuum. The shaded vertical bars indicate the wavelengths used to determine the flux ratios F_{10}/F_{12} and F_{11}/F_{12} .

Right: Flux ratios from the dust obtained after subtracting an estimated stellar contribution for the brightest sources in the AGB sample in Sloan & Price (1998). The derived flux ratios define the *Silicate Dust Sequence* (SE).

REFERENCES

- Adam, C., & Ohnaka, K. 2019, *A&A*, 628, A132, doi: [10.1051/0004-6361/201834999](https://doi.org/10.1051/0004-6361/201834999)
- Baudry, A., Wong, K. T., Etoka, S., et al. 2023, *A&A*, 674, A125, doi: [10.1051/0004-6361/202245193](https://doi.org/10.1051/0004-6361/202245193)
- Danilovich, T., Gottlieb, C. A., Decin, L., et al. 2020, *ApJ*, 904, 110
- De Beck, E., Kamiński, T., Patel, N. A., et al. 2013, *A&A*, 558, A132, doi: [10.1051/0004-6361/201321349](https://doi.org/10.1051/0004-6361/201321349)
- Decin, L. 2021, *ARA&A*, 59, 337, doi: [10.1146/annurev-astro-090120-033712](https://doi.org/10.1146/annurev-astro-090120-033712)
- Decin, L., Richards, A. M. S., Danilovich, T., Homan, W., & Nuth, J. A. 2018, *A&A*, 615, A28, doi: [10.1051/0004-6361/201732216](https://doi.org/10.1051/0004-6361/201732216)
- Decin, L., De Beck, E., Brünken, S., et al. 2010, *A&A*, 516, A69, doi: [10.1051/0004-6361/201014136](https://doi.org/10.1051/0004-6361/201014136)
- Decin, L., Richards, A. M. S., Waters, L. B. F. M., et al. 2017, *A&A*, 608, A55, doi: [10.1051/0004-6361/201730782](https://doi.org/10.1051/0004-6361/201730782)
- Decin, L., Montargès, M., Richards, A. M. S., et al. 2020, *Science*, 369, 1497
- Decin, L., Gottlieb, C., Richards, A., et al. 2022, *The Messenger*, 189, 3, doi: [10.18727/0722-6691/5283](https://doi.org/10.18727/0722-6691/5283)
- Egan, M. P., & Sloan, G. C. 2001, *ApJ*, 558, 165, doi: [10.1086/322443](https://doi.org/10.1086/322443)
- El Mellah, I., Bolte, J., Decin, L., Homan, W., & Keppens, R. 2020, *A&A*, 637, A91, doi: [10.1051/0004-6361/202037492](https://doi.org/10.1051/0004-6361/202037492)
- Esseldeurs, M., Siess, L., De Ceuster, F., et al. 2023, *A&A*, 674, A122, doi: [10.1051/0004-6361/202346282](https://doi.org/10.1051/0004-6361/202346282)
- Gobrecht, D., Hashemi, S. R., Plane, J. M. C., et al. 2023, *A&A*, 680, A18, doi: [10.1051/0004-6361/202347546](https://doi.org/10.1051/0004-6361/202347546)
- Gobrecht, D., Plane, J. M. C., Bromley, S. T., et al. 2022, *A&A*, 658, A167, doi: [10.1051/0004-6361/202141976](https://doi.org/10.1051/0004-6361/202141976)
- Gottlieb, C. A., Decin, L., Richards, A. M. S., et al. 2022, *A&A*, 660, A94, doi: [10.1051/0004-6361/202140431](https://doi.org/10.1051/0004-6361/202140431)
- Höfner, S., & Olofsson, H. 2018, *A&A Rv*, 26, 1, doi: [10.1007/s00159-017-0106-5](https://doi.org/10.1007/s00159-017-0106-5)
- Homan, W., Montargès, M., Pimpanuwat, B., et al. 2020, *A&A*, 644, A61, doi: [10.1051/0004-6361/202039185](https://doi.org/10.1051/0004-6361/202039185)
- Homan, W., Pimpanuwat, B., Herpin, F., et al. 2021, *A&A*, 651, A82, doi: [10.1051/0004-6361/202140512](https://doi.org/10.1051/0004-6361/202140512)
- Kim, H., Wyrowski, F., Menten, K. M., & Decin, L. 2010, *A&A*, 516, A68, doi: [10.1051/0004-6361/201014094](https://doi.org/10.1051/0004-6361/201014094)
- Lamers, H. J. G. L. M., & Cassinelli, J. P. 1999, *Introduction to Stellar Winds*
- Maes, S., Homan, W., Malfait, J., et al. 2021, *A&A*, 653, A25, doi: [10.1051/0004-6361/202140823](https://doi.org/10.1051/0004-6361/202140823)
- Maes, S., Van de Sande, M., Danilovich, T., De Ceuster, F., & Decin, L. 2023, *MNRAS*, 522, 4654, doi: [10.1093/mnras/stad1152](https://doi.org/10.1093/mnras/stad1152)
- Malfait, J., Homan, W., Maes, S., et al. 2021, *A&A*, 652, A51, doi: [10.1051/0004-6361/202141161](https://doi.org/10.1051/0004-6361/202141161)
- McKemmish, L. K., Masseron, T., Hoeijmakers, H. J., et al. 2019, *MNRAS*, 488, 2836, doi: [10.1093/mnras/stz1818](https://doi.org/10.1093/mnras/stz1818)
- Montargès, M., Cannon, E., de Koter, A., et al. 2023, *A&A*, 671, A96, doi: [10.1051/0004-6361/202245398](https://doi.org/10.1051/0004-6361/202245398)
- Plane, J. M. C. 2013, *Philosophical Transactions of the Royal Society of London Series A*, 371, 20120335, doi: [10.1098/rsta.2012.0335](https://doi.org/10.1098/rsta.2012.0335)
- Plane, J. M. C., & Robertson, S. H. 2022, *Faraday Discussions*, 238, 461, doi: [10.1039/D2FD00025C](https://doi.org/10.1039/D2FD00025C)
- Sloan, G. C., & Price, S. D. 1995, *ApJ*, 451, 758, doi: [10.1086/176262](https://doi.org/10.1086/176262)
- . 1998, *ApJS*, 119, 141, doi: [10.1086/313156](https://doi.org/10.1086/313156)
- Van de Sande, M., & Millar, T. J. 2022, *MNRAS*, 510, 1204, doi: [10.1093/mnras/stab3282](https://doi.org/10.1093/mnras/stab3282)
- Wallström, S. H. J., Danilovich, T., Müller, H. S. P., et al. 2024, *A&A*, 681, A50, doi: [10.1051/0004-6361/202347632](https://doi.org/10.1051/0004-6361/202347632)

ATOMIUM Publications:

ATOMIUM Large Program

- Pimpanuwat B., Gray, M., Etoka, S., et al. "ATOMIUM: Investigating the innermost regions of oxygen rich circumstellar envelopes with ALMA observations of millimeter wavelength SiO masers", in preparation
- Wallström, S. H. J., Danilovich, T., Müller, H.S.P., et al. "ATOMIUM: Molecular inventory of 17 oxygen rich evolved stars observed with ALMA", 2023, 2024, A&A, 681, A50 doi:10.1051/0004-6361/202347632
- Danilovich, T., Malfait, J., Van de Sande, M., et al. "Chemical tracers of a highly eccentric binary orbit", 2024, Nature Astronomy, doi:10.1038/s41550-023-02154-y
- Baudry, A., Wong, K. T., Etoka, S., et al. "ATOMIUM: Probing the inner wind of evolved O-rich stars with new, highly excited H₂O and OH lines", 2023, A&A, 674, A125 doi:10.48550/arXiv.2305.03171
- Montargès, M., Cannon, E., de Koter, A., et al. "The VLT/SPHERE view of the ATOMIUM cool evolved star sample: I. Overview: Sample characterization through polarization analysis", 2023, A&A, 671, A96 doi:10.1051/0004-6361/202245398
- Decin, L., Gottlieb, C., Richards, A., et al. "ATOMIUM: ALMA Tracing the Origins of Molecules In dUst forming oxygen-rich M-type stars", 2022, The Messenger, 189, 3 doi:10.18727/0722-6691/5283
- Gottlieb, C. A., Decin, L., Richards, A. M. S., et al. "ATOMIUM: ALMA tracing the origins of molecules in dust forming oxygen rich M-type stars: Motivation, sample, calibration, and initial results", 2022, A&A, 660, A94 doi:10.1051/0004-6361/202140431
- Danilovich, T., Van de Sande, M., Plane, J. M. C., et al. "ATOMIUM: halide molecules around the S-type AGB star W Aquilae", 2021, A&A, 655, A80 doi:10.1051/0004-6361/202141757
- Homan, W., Pimpanuwat, B., Herpin, F., et al. "ATOMIUM: The astounding complexity of the near circumstellar environment of the M-type AGB star R Hydrae: I. Morpho-kinematical interpretation of CO and SiO emission", 2021, A&A, 651, A82 doi:10.1051/0004-6361/202140512
- Homan, W., Montargès, M., Pimpanuwat, B., et al. "ATOMIUM: A high-resolution view of the highly asymmetric wind of the AGB star π^1 Gruis: I. First detection of a new companion and its effect on the inner wind", 2020, A&A, 644, A61 doi:10.1051/0004-6361/202039185
- Decin, L., Montargès, M., Richards, A. M. S., et al. "(Sub)stellar companions shape the winds of evolved stars", 2020, Science, 369, 1497 doi:10.1126/science.abb1229

ATOMIUM Pilot

- Decin, L. "Evolution and Mass Loss of Cool Ageing Stars: a Daedalean Story", 2021, Annu. Rev. Astron. Astrophys., 59, 337 doi: 10.1146/annurev-astro-090120-033712
- Danilovich, T., Gottlieb, C. A., Decin, L., et al. "Rotational Spectra of Vibrationally Excited AlO and TiO in Oxygen-rich Stars", 2020, ApJ, 904, 110 doi:10.3847/1538-4357/abc079
- Decin, L.; Richards, A. M. S.; Danilovich, T., et al. "ALMA spectral line and imaging survey of a low and a high mass-loss rate AGB star between 335 and 362 GHz", 2018, A&A, 615, A28 doi:10.1051/0004-6361/201732216
- Decin, L.; Richards, A. M. S.; Waters, L. B. F. M., et al. "Study of the aluminium content in AGB winds using ALMA Indications for the presence of gas-phase (Al₂O₃)_n clusters", 2017, A&A, 608, A55 doi:10.1051/0004-6361/201730782
- Homan, W., Boulanger, J., Decin, L., and de Koter, A. "Simplified models of circumstellar morphologies for interpreting high-resolution data. Analytical approach to the equatorial density enhancement", 2016, A&A, 596, A91 doi:10.1051/0004-6361/201528000

ATOMIUM Motivated

Chemistry

- Gobrecht, D., Hashemi, S. R., Plane, J. M. C., et al., "Bottom-up dust nucleation theory in oxygen-rich evolved stars. II. Magnesium and calcium aluminate clusters", 2023, A&A, 680, A18 doi:10.1051/0004-6361/202347546
- Maes, S.; Van de Sande, M.; Danilovich, T. et al., "Sensitivity study of chemistry in AGB outflows using chemical kinetics", 2023, MNRAS, 522, 4654 doi:10.1093/mnras/stad1152
- Gobrecht, D., Plane, J. M. C., Bromley, S. T., et al., "Bottom-up dust nucleation theory in oxygen-rich evolved stars. I. Aluminum oxide clusters". 2022, A&A, 658, 167 doi:10.1051/0004-6361/202141976

Van de Sande, M. and Millar, T. J., "The impact of stellar companion UV photons on the chemistry of the circumstellar environments of AGB stars", 2022, MNRAS, 510, 1204 doi:10.1093/mnras/stab3282

Douglas, K. M., Gobrecht, D., Plane, J. M. C., "Experimental study of the removal of excited state phosphorus atoms by H₂O and H₂: implications for the formation of PO in stellar winds", 2022, MNRAS, 515, 99 doi:10.1093/mnras/stac1684

Plane, J. M. C., and Robertson, S. H., "Master equation modelling of non-equilibrium chemistry in stellar outflows", 2022, Faraday Discuss., 238, 461 doi:10.1039/D2FD00025C

Hydrodynamical simulations

Siess, L., Homan, W., Toupin, S., et al. "3D simulations of AGB stellar winds. I. Steady winds and dust formation", 2022, A&A, 667, A75 doi:10.1051/0004-6361/202243540

Maes, S., Homan, W., Malfait, J., et al., "SPH modelling of companion-perturbed AGB outflows including a new morphology classification scheme", 2021, A&A, 653, A25 doi:10.1051/0004-6361/202140823

Malfait, J., Homan, W., Maes, S., et al., "SPH modelling of wind-companion interactions in eccentric AGB binary systems", 2021, A&A, 652, A51 doi:10.1051/0004-6361/202141161

El Mellah, I., Bolte, J., Decin, L., et al., "Wind morphology around cool evolved stars in binaries. The case of slowly accelerating oxygen-rich outflows", 2020, A&A, 637, A91 doi:10.1051/0004-6361/202037492